SAND2015-9606J

Enhanced Thermoelectric Transport in Modulation-Doped GaN/AlGaN Core/Shell Nanowires

Erdong Song[1], Qiming Li[2], Brian Swartzentruber[3], Wei Pan[2], George T. Wang[2*], Julio A. Martinez[1*]

[1] Department of Chemical & Materials Engineering, New Mexico State University, Las Cruces, NM 88003, USA.
[2] Sandia National Laboratories, Albuquerque, NM 87123, USA.
[3] Center for Integrated Nanotechnologies, Sandia National Laboratories, Albuquerque, NM 87185, USA.

The thermoelectric properties of unintentionally n-doped core GaN/AlGaN core/shell N-face nanowires are reported. We found that the temperature dependence of the electrical conductivity is consistent with thermally activated carriers with two distinctive donor energies. The Seebeck coefficient of GaN/AlGaN nanowires is more than twice larger than that for the GaN nanowires alone. However, an outer layer of GaN deposited onto the GaN/AlGaN core/shell nanowires decreases the Seebeck coefficient at room temperature while the temperature dependence of the electrical conductivity remains the same. We attribute these observations to the formation of an electron gas channel within the heavily-doped GaN core of the GaN/AlGaN nanowires. The room-temperature thermoelectric power factor for the GaN/AlGaN nanowires can be four times higher than the GaN nanowires. Selective doping in bandgap engineered core/shell nanowires is proposed for enhancing the thermoelectric power.

Keywords: GaN, AlGaN, Seebeck coefficient, electron gas, hole gas.

1. Introduction

One of the distinctive features of band-gap engineered heterostructured nanowires and thin films is the presence a carrier gas layer with high mobilities [1-4], which is highly desirable for field effect transistors [5-7], for solar cells in order to minimize carrier recombination [8], and for thermoelectrics with the objective of enhancing the thermoelectric power factor[9]. In general, researchers have focused on the study and understanding of undoped band-gap engineered nanostructures because of the notion that extrinsic doping would defeat the large carrier mobility of the carrier-gas layer [2, 10]. However, in some cases, doped band-gap engineered nanostructured materials have been explored as an approach to modulate the electronic properties [11].

Decreasing the thermal conductivity via phonon-boundary scattering events in semiconductor nanowires has helped achieve thermal conductivities comparable to amorphous materials, thus improving the thermoelectric figure of merit, $ZT = S^2T(\sigma/k)$, in which S is the Seebeck coefficient, T is the absolute temperature, σ is the electrical conductivity, and k is the thermal conductivity [9, 12, 13]. In addition to increasing phonon-scattering, a larger ZT can be achieved by increasing the Seebeck coefficient (ZT is proportional to S^2). However, gains in S are generally offset by a corresponding reduction in σ resulting in a lower power factor ($S^2\ \sigma$). Decoupling the opposing effects of S and σ has been elusive despite extensive work in the field of thermoelectrics. S and σ was proposed to be decoupled in band-engineered nanowires due to the large mobility of carriers without the need to extrinsically dope, but this approach has not yet yielded the expected increase of $S^2\ \sigma$ [4]. Quantum confinement in small diameter

nanowires could provide another alternative for increasing $S^2\sigma$, but due to nanowire diameter restrictions the thermal broadening and overlapping of the sub-band energies limited this approach to temperatures below 100 K [14].

In this work, we measured the thermoelectric properties of unintentionally-doped n-type GaN, unintentionally-doped core GaN/AlGaN core/shell, and GaN/AlGaN/GaN core/shell/shell nanowires (NWs). In all cases, we found that the GaN NW (core) provides a degenerate and a thermally activated conduction channels. The growth of a shell provides an additional thermally activated conduction channel. The GaN/AlGaN core/shell NWs have a substantially larger *S* than the GaN NW. However, the addition of the extra GaN shell results in a decreasing *S* with increasing temperature.

2. Experimental Methods

Unintentionally doped n-type GaN NWs were grown by metal-organic chemical vapor deposition (MOCVD) at ~900 °C on *r*-plane sapphire using thin Ni films deposited by e-beam evaporation as a catalyst for vapor-liquid-solid (VLS) growth, as described previously [15-17]. The NWs grow along the [11-20] direction with triangular cross-sections comprised of a (000-1) facet and two {1-101} facets. GaN/AlGaN core/shell NWs were grown separately by following the GaN NW growth process *in-situ* with MOCVD deposition of an AlGaN shell layer at ~1050 °C [18]. Cross-section scanning transmission electron microscopy images show AlGaN shell thicknesses ranging from 10 – 35 nm thick (Figure 1A) with Al content from ~20 – 30% as determined by energy dispersive spectroscopy. GaN/AlGaN/GaN core/shell/shell NWs were synthetized by

subsequently depositing a GaN shell layer onto the AlGaN shell layer. The NWs were typically tapered with dimensions of 150 nm - 250 nm base width and more than 15 µm long. The thermoelectric characterization platform was produced by standard photolithography methods on a 1000 nm thick LPCVD silicon nitride on silicon substrate. E-beam metal evaporation was performed to sequentially deposit 5 nm Ti, 50 nm Au, 30 nm Ti, 100 nm of Al, and 20 nm Ti followed by metal lift-off in acetone for about 4 hours. Single NWs were picked from the as-grown substrate and placed on the thermoelectric characterization platform by a nanomanipulator tool developed by our group [12]. E-beam lithography was carried out to pattern contact lines on top of the nanowires in order to achieve good electrical and thermal contacts. E-beam metal evaporation of 80 nm Ti (first layer), 80 nm of Al, 20 nm of Ti, and 30 nm of Au were carried out after PMMA development. Finally, lift-off of the E-beam resist was carried out in acetone, followed by rapid thermal annealing (RTA) at 750 ^{o}C for 30 seconds in forming gas (5% H_2 in N_2), which yielded ohmic contacts for the devices. This procedure produced nanowires suspended between contacts (Figure 1B).

Samples were tested in a probe station, and later mounted in a helium closed-loop cryostat. 4-probe AC electrical resistance (R_{4probe}) was measured from 25 K to 310 K at 13 Hz. Contacts were ohmic within the studied temperature range. The electrical resistivity (ρ) for our triangular cross section tapered nanowire was calculated from $\rho = R_{4probe} \times (\sqrt{3} / 4) \times (d_3 \times d_4 / l_{3-4})$, where d_3 and d_4 are the width of the nanowire at the contacts 3 and 4 respectively, and l_{3-4} is the length between them (Figure 1 B). The dimensions of the nanowire were measured by HRSEM. The Seebeck coefficient

(S=-$\Delta V_{th}/\Delta T$) of our nanowires was extracted by measuring the thermal voltage, ΔV_{th}, and the temperature difference, ΔT, between leads 3 and 4 when a DC current was applied to the heater (lead 1) (Figure 1B) [19, 20]. Measurements were taken at a pressure of 5 x 10^{-6} Torr or lower.

3. Results and Discussion

3.1 Electronic Transport of III-Nitrogen NWs

The understanding of the thermoelectric characteristics of a material is greatly simplified by the formation of ohmic contacts between the test leads and the sample under study. Figure 2A shows a typical ohmic I-V characterization curve for our III-Nitrogen NWs at 25 K and 300 K. Ohmic contacts were realized after RTA for every device employed in this study. The contact resistivity (Figure 2B) increases as the temperature decreases which indicates a thermal activated process. During RTA, a highly conductive TiN layer forms at the Ti-GaN interface [21] by the extraction of gallium atoms of the crystal matrix and replacement by titanium atoms. The formation of TiN during RTA creates a small energetic barrier between the metal contacts and n-type GaN with the barrier height inversely proportional to the carrier concentration of the GaN [22]. As the temperature decreases, the carrier concentration of GaN decreases (Figure 3) increasing the contact barrier height, so electrical contacts become more resistive. For the Ti-AlGaN interface, titanium can only replace gallium during RTA because of a strong Al-N bond, but ohmic characteristics are still observed [21]. A highly defective Al-Ti-N phase should form at the metal-GaN/AlGaN core/shell nanowire after

RTA. The contact resistivity of GaN NW turned out to be about 2 orders of magnitude smaller than the one for GaN/AlGaN NW while the 4-probe electrical conductivities are comparable among the nanowires (Figure 3). Our contact resistivities indicate that we realized electrical contact to the AlGaN shell of GaN/AlGaN NWs. The temperature dependence of the GaN/AlGaN contact resistivity is similar to the one for GaN NW, so the contact barrier height could also be dependent of the carrier concentration in GaN/AlGaN NWs.

The electrical conductivity as function of temperature for the different samples is shown in Figure 3. We find the GaN NW has a relatively large electrical conductivity, whereas undoped GaN is reported to be highly resistive [1, 2, 23]. Unintentional doping during growth is likely the reason behind this observation [6, 23-26]. The Seebeck coefficient (Figure 4) of the GaN NW is negative indicating the presence of electron donors. The electrical conductivities versus temperature have the characteristic behavior of a thermally activated process (Figure 3). At T < 50 K, the conductivities of GaN are essentially degenerate which indicates the presence of a temperature independent conduction channel. Therefore, the conductivity data for GaN and core/shell nanowires were fitted with either a single exponential (eq. 1) or double exponential decay (eq. 2) with a degenerate conduction term (σ_0) [27]. k_B is the Boltzmann constant and T is the absolute temperature.

$$\sigma(T) = \sigma_0 + \sigma_1 \exp(-E_{a1}/k_B T) \quad (1)$$

$$\sigma(T) = \sigma_0 + \sigma_1 \exp(-E_{a1}/k_B T) + \sigma_2 \exp(-E_{a2}/k_B T) \quad (2)$$

The activation energies (E_{a1}, E_{a2}) and temperature independent conductivities (σ_0, σ_1, and σ_2) for eq. 1 and 2 are reported in Table 1. The activation energies for the GaN nanowires with eq. 1 are (18.7 ± 1.1) meV and (31.8 ± 0.9) meV. The use of eq. 2 for the GaN nanowires yields E_{a1} and E_{a2} which are not consistent with previously reported values for conductive GaN [10, 27, 28]. A second shallow thermally activated conduction channel ($E_a \approx$ 2 – 6 meV) was reported in some cases for unintentionally doped GaN [27] which is not observed for our GaN nanowire. The synthesis process is known to influence the electronic properties of unintentionally doped GaN nanowires [26, 28, 29]. The large temperature-independent conduction channel (σ_0) observed in our GaN and GaN core nanowires and its relatively large variation among the samples could be the associated with our synthesis process. The activation energy found by eq. 1 is similar to that reported for substitutional oxygen impurities in doped GaN [25, 30], so it leads us to assume that our GaN nanowires were unintentionally doped with oxygen during growth.

Table 1. Fitting parameters for the conductivity of GaN, GaN/AlGaN, and GaN/AlGaN/GaN nanowires.

	σ_0 (S/cm)	σ_1 (S/cm)	E_{a1} (meV)	σ_2 (S/cm)	E_{a2} (meV)
GaN #1	90.1 ± 0.2	90.7 ± 3.5	31.8 ± 0.9	-	-
GaN #2	264.1 ± 0.5	64.3 ± 3.1	18.7 ± 1.1	-	-
GaN/AlGaN #1	43.4 ± 0.2	77.0 ± 0.8	34.5 ± 0.6	12.4 ± 0.5	5.4 ± 0.4
GaN/AlGaN #2	37.3 ± 0.5	36.3 ± 0.1	28.3 ± 0.0	4.6 ± 0.3	3.0 ± 0.0
GaN/AlGaN #3	78.6 ± 0.4	44.0 ± 1.1	28.1 ± 1.7	16.5 ± 1.5	5.6 ± 0.8
GaN/AlGaN/GaN #1	31.2 ± 0.2	35.3 ± 0.8	34.9 ± 1.2	10.9 ± 0.2	4.8 ± 0.4
GaN/AlGaN/GaN #2	30.6 ± 1.1	14.8 ± 0.4	13.3 ± 1.1	10.8 ± 1.0	1.4 ± 0.8

Errors represent 95% confidence interval of the fitting parameters

The electrical conductivities of GaN/AlGaN core/shell and GaN/AlGaN/GaN core/shell/shell NWs showed a similar temperature trend as the GaN NW (Figure 3). The fitting of σ data in Figure 3 for both types of nanowires with eq. 2 yields two distinct donor activation energies (Table 1). A single activation energy cannot fit either nanowire over the entire temperature range. Since E_{a1} energies found for the GaN/AlGaN and GaN/AlGaN/GaN NWs are similar to the activation energies for GaN, we conclude that the electronic properties of the heavily doped GaN core are still contributing to the electronic transport of GaN/AlGaN and GaN/AlGaN/GaN NWs. An electron gas (EG) conduction channel with phonon-electron scattering characteristics and carrier concentration independent of the temperature was observed in undoped GaN/AlGaN NWs [2] and thin films [10]. However, E_{a2} for GaN/AlGaN and GaN/AlGaN/GaN samples were estimated to be 1 – 5 meV indicating a shallow conduction channel that is not observed in our GaN NWs.

The shallow thermal activated conduction channel (E_{a2}) observed for our GaN/AlGaN NWs does not correlate with previously reported EG characteristics. The presence of an EG channel in triangular N-face GaN/AlGaN doped-core/doped-shell NWs has been theoretically predicted [3], and doped-GaN/doped-AlGaN thin films showed an electron mobility and a sheet carrier concentration dictated by the 2-DEG [10]. However, the electron gas channel in large diameter N-face GaN/AlGaN NWs is less confined compared to small nanowires [3]. Furthermore, oxygen doping in GaN/AlGaN thin films is associated with the large EG carrier concentration [31]. The Fermi energy level and EG confinement is also influenced by the oxygen donor concentration [32].

Thermoelectric characteristics of non-confined EG in GaN/AlGaN are yet to be reported. However, the hole concentration for a three dimensional hole gas (3DHG) in a Mg-graded AlGaN layer on GaN was reported to slowly decay with decreasing temperature [33, 34]. The second shallow channel in our nanowires may indicate an electron gas with low degree of confinement as a result of the dimensions of the GaN/AlGaN and GaN/AlGaN/GaN NWs and the donor concentration of the GaN core.

3.2 Seebeck Coefficient of III-Nitrogen NWs

Another important aspect of the GaN/AlGaN NWs is the contribution of the shallow channel to the overall Seebeck coefficient. S versus T for our samples is shown in Figure 4. At 300 K, $S \approx$ -72 x 10^{-6} V/K was measured for the GaN NW (S_{GaN}). S decreases as T decreases with a similar trend to the one reported for heavily doped ($n_{GaN} \approx$ 6.6 x 10^{19} cm^{-3}) n-type GaN NWs [20]. Based on the single band model [35], we estimate $n_{GaN} \approx$ 1.3 x 10^{19} cm^{-3} (assuming an effective electron mass equal to 0.22 m_e [36]) indicating a large donor concentration in our GaN NW. The observed Seebeck coefficient for the GaN/AlGaN NWs ($S_{GaN/AlGaN}$) is also negative (n-type) and more than twice larger than S_{GaN} within the measured temperature range. For two independent parallel conduction channels [12], $S_{GaN/AlGaN}$ should have contributions from the heavily doped GaN core and the shallow conduction channel. Thus assuming that S_{GaN} remains the same after AlGaN shell deposition, our experimental data indicate that the shallow channel contributes a substantially large S to the overall increase of $S_{GaN/AlGaN}$. Increasing the Seebeck coefficient by field gate modulation of carrier concentration [4, 37], by field gate carrier

confinement [38], and by thin film band engineered 2-DEG carrier confinement [39] has been explored. However, increasing the Seebeck coefficient by doping the core of core/shell nanowires has not been previously reported. The large $S_{GaN/AlGaN}$ due to the contribution of the shallow channel for our GaN/AlGaN core/shell Nws could be a consequence of an electron gas channel increasing the energy dependence of the density of states ($dn(E)/dE$) [38, 39].

To gain further insight into the electron transport in our GaN/AlGaN NWs we carried out studies with GaN/AlGaN/GaN core/shell/shell NWs. While σ versus T shows a similar trend with GaN/AlGaN (Figure 3), the Seebeck coefficient of GaN/AlGaN/GaN ($S_{GaN/AlGaN/GaN}$) differs significantly from $S_{GaN/AlGaN}$ between 180 K and 300 K (Figure 4). The influence of the outer GaN shell to $S_{GaN/AlGaN/GaN}$ is considered thermally dependent. From 25 K to 180 K, $S_{GaN/AlGaN/GaN}$ is similar to $S_{GaN/AlGaN}$ while $S_{GaN/AlGaN/GaN}$ at 300 K was found to be comparable to S_{GaN}, so the enhancement of $S_{GaN/AlGaN}$ seems to be eliminated after the deposition of the GaN outer shell.

Coating a GaN/AlGaN thin film with a GaN film (GaN/AlGaN/GaN) results in the formation of a 2-dimensional hole gas (2DHG) layer at the AlGaN/GaN interface due to fixed polarization charges induced by the 2DEG layer in the GaN/AlGaN [40-42]. Similarly, the non-confined electron gas layer within the core of GaN/AlGaN NWs could induce the formation of a hole gas (HG) layer in GaN/AlGaN/GaN NWs. During thermal voltage measurements, the diffusion of holes in the hole-gas channel opposes the diffusion of electrons in the EG leading to a smaller $S_{GaN/AlGaN/GaN}$. The curvature of $S_{GaN/AlGaN/GaN}$ versus temperature indicates that the Seebeck contribution of the HG layer is reduced

at low temperature range. Equation 3 provides the relation between the observed Seebeck coefficient and it components where $G_{GaN/AlGaN}$, $G_{GaN/AlGaN/GaN}$, and G_{HG} are the conductance of the GaN/AlGaN, GaN/AlGaN/GaN, and HG respectively. The Seebeck coefficient expression by the Cutler-Mott [43] is employed to capture the overall Seebeck behavior where e is the electron charge, E_f is the Fermi energy level, and B is the dimensional constant between G_{HG} and the conductivity of HG (σ_{HG}).

$$S(T) = \frac{G_{Gan/AlGaN}}{G_{Gan/AlGaN/GaN}} S_{Gan/AlGaN} + \frac{G_{HG}}{G_{Gan/AlGaN/GaN}} S_{HG} \quad (3)$$
$$= A\,T + \frac{B * \sigma_{HG}}{G_{Gan/AlGaN/GaN}} \frac{\pi^2\, k_B^2\, T}{3\, e} \left(\frac{1}{\sigma_{HG}} \frac{d\sigma_{HG}}{dE} \right) \Big|_{E_f}$$

Based on $S_{GaN/AlGaN}$ data in Figure 4, the first term of the right hand side of eq. 3 can be approximated to a linear relation of T where A is a constant. From 25 K to 140 K, $S_{GaN/AlGaN/GaN}$ turned out to be a linear function of the absolute temperature. Assuming the contribution of the HG to $S_{GaN/AlGaN/GaN}$ is not negligible, our observation indicates that $(d\sigma_{HG}/dE)_{Ef}/G_{GaN/AlGaN/GaN}$ should be constant. It turns out that $G_{GaN/AlGaN/GaN}$ is a weak function of the temperature (Figure 3), and the HG carrier concentration ($n_{HG}(E,T)$) and mobility ($\mu_{HG}(E,T)$) are not expected to change from 25 K to 140 K [42], so the slope of $S_{GaN/AlGaN/GaN}$ versus T contains the linear contributions of electrons and holes. For temperatures higher than 140 K, $S_{GaN/AlGaN/GaN}$ shows a larger and nonlinear contribution of holes. Increasing the carrier concentration of thermally active oxygen donors moves the Fermi energy level deeper into the conduction band of the GaN core turning into a larger EG carrier concentration [32]. Based on electrical conductivity data (figure 3), the

concentration of oxygen active donor sites in the GaN core of our nanowires exponentially increases becoming predominant for T higher than 140 K. Therefore, a concentration increase of EG is expected resulting in a larger positive polarization at the GaN/AlGaN core/shell interface which it should increase the negative polarization charges at the AlGaN/GaN shell/outer-shell interface. Thus a larger HG concentration is reasonable, but the upward change of E_f could result only in a modest gain of the HG concentration. The electrical conductivities for GaN/AlGaN/GaN nanowires have a similar temperature trend to the conductivities of GaN/AlGaN samples supporting a modest gain of HG concentration. Therefore, the nonlinear increase of the second right hand side term of eq. 3 should have other contributions besides σ_{HG} gain. The Seebeck coefficient of an EG can be substantially increased by a positive electric field due to EG layer confinement [38]. Similarly, the increase of the positive polarization charge density at the AlGaN/GaN shell/outer-shell interface should also yield a more confined HG layer resulting in a larger S_{HG}.

4. Conclusions

We report the formation of a shallow electron channel in N-face unintentionally doped n-type core GaN/AlGaN core/shell NWs. Electrical conductivity and Seebeck coefficient measurements of GaN/AlGaN NWs indicate that the shallow electron channel could be the result of a non-confined electron gas channel. Furthermore, GaN/AlGaN/GaN doped-core/shell/shell NWs show a Seebeck coefficient trend that supports the formation of a hole gas due to the presence of an EG channel in the GaN/AlGaN

core/shell. Due to the enhanced Seebeck coefficient of GaN/AlGaN NWs, the resulting thermoelectric power factor at 300 K ($S^2\sigma$) is about 4 times larger than GaN NWs (2.4 x 10^{-4} W/m-K^2 and 0.62 x 10^{-4} W/m-K^2 for GaN/AlGaN and GaN NWs respectively). Even though the heavily doped core still dominates the electrical conductivity, the EG channel substantially contributes to the overall Seebeck coefficient. We propose enhancement of ZT by a heavily doped GaN core and size reduction to increase the confinement of the EG channel.

Acknowledgement

This work was supported by the U.S. Department of Energy, Office of Science, Basic Energy Sciences, Materials Sciences and Engineering Division and by the New Mexico State University through startup funding to Professor Martinez. We thank François Leonard for a critical reading of the manuscript and helpful discussions. This work was performed, in part, at the Center for Integrated Nanotechnologies, an Office of Science User Facility operated for the U.S. Department of Energy (DOE) Office of Science by Los Alamos National Laboratory (Contract DE-AC52-06NA25396) and Sandia National Laboratories (Contract DE-AC04-94AL85000). Sandia National Laboratories is a multi-program laboratory managed and operated by Sandia Corporation, a wholly owned subsidiary of Lockheed Martin Corporation, for the U.S. Department of Energy's National Nuclear Security Administration under contract DE-AC04-94AL85000.

References

[1] Acar S, Lisesivdin S B, Kasap M, Özçelik S, Özbay E 2008 Determination of two-dimensional electron and hole gas carriers in AlGaN/GaN/AlN heterostructures grown by Metal Organic Chemical Vapor Deposition *Thin Solid Films* 516 2041-4.

[2] Li Y, Xiang J, Qian F, Gradečak S, Wu Y, Yan H, Blom D A, Lieber C M 2006 Dopant-Free GaN/AlN/AlGaN Radial Nanowire Heterostructures as High Electron Mobility Transistors *Nano Lett.* 6 1468-73.

[3] Wong B M, Leonard F, Li Q, Wang G T 2011 Nanoscale effects on heterojunction electron gases in GaN/AlGaN core/shell nanowires *Nano Lett* 11 3074-9.

[4] Moon J, Kim J H, Chen Z C, Xiang J, Chen R 2013 Gate-modulated thermoelectric power factor of hole gas in Ge-Si core-shell nanowires *Nano Lett* 13 1196-202.

[5] Goldhaber-Gordon D, Shtrikman H, Mahalu D, Abusch-Magder D, Meirav U, Kastner M A 1998 Kondo effect in a single-electron transistor *Nature* 391 156-9.

[6] Khan M A, Bhattarai A, Kuznia J N, Olson D T 1993 High electron mobility transistor based on a GaN-Al[sub x]Ga[sub 1 - x]N heterojunction *Appl. Phys. Lett.* 63 1214.

[7] Kaun S W, Wong M H, Dasgupta S, Choi S, Chung R, Mishra U K, Speck J S 2011 Effects of Threading Dislocation Density on the Gate Leakage of AlGaN/GaN Heterostructures for High Electron Mobility Transistors *Appl. Phys. Express* 4 024101.

[8] Westphalen M, Kreibig U, Rostalski J, Lüth H, Meissner D 2000 Metal cluster enhanced organic solar cells *Sol. Energ. Mat. Sol. C.* 61 97-105.

[9] Tritt T M 2011 Thermoelectric Phenomena, Materials, and Applications *Ann. Rev. Mater. Res.* 41 433-48.

[10] Dziuba Z, Antoszewski J, Dell J M, Faraone L, Kozodoy P, Keller S, Keller B, DenBaars S P, Mishra U K 1997 Magnetic field dependent Hall data analysis of electron transport in modulation-doped AlGaN/GaN heterostructures *J. Appl. Phys.* 82 2996.

[11] Dillen D C, Kim K, Liu E-S, Tutuc E 2014 Radial modulation doping in core-shell nanowires *Nat. Nanotechnol.* 9 116-20.

[12] Martinez J A, Cho J-H, Liu X, Luk T S, Huang J, Picraux S T, Sullivan J P, Swartzentruber B S 2013 Contribution of radial dopant concentration to the thermoelectric properties of core-shell nanowires *Appl. Phys. Lett.* 102 103101.

[13] Pantha B N, Dahal R, Li J, Lin J Y, Jiang H X, Pomrenke G 2008 Thermoelectric properties of In[sub x]Ga[sub 1−x]N alloys *Appl. Phys. Lett.* 92 042112.

[14] Tian Y, Sakr M R, Kinder J M, Liang D, MacDonald M J, Qiu R L J, Gao H-J, Gao X P A 2012 One-Dimensional Quantum Confinement Effect Modulated Thermoelectric Properties in InAs Nanowires *Nano Lett.* 12 6492-7.

[15] Wang G T, Talin A A, Werder D J, Creighton J R, Lai E, Anderson R J, Arslan I 2006 Highly aligned, template-free growth and characterization of vertical GaN nanowires on sapphire by metal–organic chemical vapour deposition *Nanotechnology* 17 5773.

[16] Li Q, Wang G T 2008 Improvement in aligned GaN nanowire growth using submonolayer Ni catalyst films *Appl. Phys. Lett.* 93 043119.

[17] Armstrong A, Li Q, Bogart K, Lin Y, Wang G, Talin A 2009 Deep level optical spectroscopy of GaN nanorods *J. Appl. Phys.* 106 053712--7.

[18] Armstrong A, Li Q, Lin Y, Talin A, Wang G 2010 GaN nanowire surface state observed using deep level optical spectroscopy *Appl. Phys. Lett.* 96 163106.

[19] Martinez J A, Provencio P P, Picraux S T, Sullivan J P, Swartzentruber B S 2011 Enhanced thermoelectric figure of merit in SiGe alloy nanowires by boundary and hole-phonon scattering *J. Appl. Phys.* 110 074317.

[20] Lee C-H, Yi G-C, Zuev Y M, Kim P 2009 Thermoelectric power measurements of wide band gap semiconducting nanowires *Appl. Phys. Lett.* 94 022106.
[21] Van Daele B, Van Tendeloo G, Ruythooren W, Derluyn J, Leys M, Germain M 2005 The role of Al on Ohmic contact formation on n-type GaN and AlGaN／ GaN *Appl. Phys. Lett.* 87 061905.
[22] Lu C, Chen H, Lv X, Xie X, Mohammad S N 2002 Temperature and doping-dependent resistivity of Ti/Au/Pd/Au multilayer ohmic contact to n-GaN *J. Appl. Phys.* 91 9218-24.
[23] Armstrong A, Li Q, Lin Y, Talin A A, Wang G T 2010 GaN nanowire surface state observed using deep level optical spectroscopy *Appl. Phys. Lett.* 96 163106.
[24] Götz W, Johnson N M, Chen C, Liu H, Kuo C, Imler W 1996 Activation energies of Si donors in GaN *Appl. Phys. Lett.* 68 3144.
[25] Meister D, Böhm M, Topf M, Kriegseis W, Burkhardt W, Dirnstorfer I, Rösel S, Farangis B, Meyer B K, Hoffmann A, Siegle H, Thomsen C, Christen J, Bertram F 2000 A comparison of the Hall-effect and secondary ion mass spectroscopy on the shallow oxygen donor in unintentionally doped GaN films *J. Appl. Phys.* 88 1811.
[26] Kim J-R, So H M, Park J W, Kim J-J, Kim J, Lee C J, Lyu S C 2002 Electrical transport properties of individual gallium nitride nanowires synthesized by chemical-vapor-deposition *Appl. Phys. Lett.* 80 3548-50.
[27] Yoon J, Girgis A M, Shalish I, Ram-Mohan L R, Narayanamurti V 2009 Size-dependent impurity activation energy in GaN nanowires *Appl. Phys. Lett.* 94 142102.
[28] Motayed A, Davydov A V, Mohammad S N, Melngailis J 2008 Experimental investigation of electron transport properties of gallium nitride nanowires *J. Appl. Phys.* 104 024302.
[29] Stern E, Cheng G, Cimpoiasu E, Klie R, Guthrie S, Klemic J, Kretzschmar I, Steinlauf E, Turner-Evans D, Broomfield E, Hyland J, Koudelka R, Boone T, Young M, Sanders A, Munden R, Lee T, Routenberg D, Reed M A 2005 Electrical characterization of single GaN nanowires *Nanotechnology* 16 2941-53.
[30] Götz W, Johnson N M, Chen C, Liu H, Kuo C, Imler W 1996 Activation energies of Si donors in GaN *Appl. Phys. Lett.* 68 3144-6.
[31] Jang H W, Jeon C M, Kim K H, Kim J K, Bae S-B, Lee J-H, Choi J W, Lee J-L 2002 Mechanism of two-dimensional electron gas formation in AlxGa1−xN/GaN heterostructures *Appl. Phys. Lett.* 81 1249-51.
[32] Chu R M, Zhou Y G, Zheng Y D, Han P, Shen B, Gu S L 2001 Influence of doping on the two-dimensional electron gas distribution in AlGaN/GaN heterostructure transistors *Appl. Phys. Lett.* 79 2270-2.
[33] Zhang L, Ding K, Yan J C, Wang J X, Zeng Y P, Wei T B, Li Y Y, Sun B J, Duan R F, Li J M 2010 Three-dimensional hole gas induced by polarization in (0001)-oriented metal-face III-nitride structure *Appl. Phys. Lett.* 97 062103.
[34] Simon J, Protasenko V, Lian C, Xing H, Jena D 2010 Polarization-induced hole doping in wide–band-gap uniaxial semiconductor heterostructures *Science* 327 60-4.
[35] Zhou F, Szczech J, Pettes M T, Moore A L, Jin S, Shi L 2007 Determination of Transport Properties in Chromium Disilicide Nanowires via Combined Thermoelectric and Structural Characterizations *Nano Lett.* 7 1649-54.
[36] Ambacher O, Smart J, Shealy J, Weimann N, Chu K, Murphy M, Schaff W, Eastman L, Dimitrov R, Wittmer L 1999 Two-dimensional electron gases induced by spontaneous and piezoelectric polarization charges in N-and Ga-face AlGaN/GaN heterostructures *J. Appl. Phys.* 85 3222-33.

[37] Roddaro S, Ercolani D, Safeen M A, Suomalainen S, Rossella F, Giazotto F, Sorba L, Beltram F 2013 Giant Thermovoltage in Single InAs Nanowire Field-Effect Transistors *Nano Lett.* 13 3638-42.
[38] Ohta H, Mizuno T, Zheng S, Kato T, Ikuhara Y, Abe K, Kumomi H, Nomura K, Hosono H 2012 Unusually large enhancement of thermopower in an electric field induced two-dimensional electron gas *Adv. Mater.* 24 740-4.
[39] Ohta H, Kim S, Mune Y, Mizoguchi T, Nomura K, Ohta S, Nomura T, Nakanishi Y, Ikuhara Y, Hirano M, Hosono H, Koumoto K 2007 Giant thermoelectric Seebeck coefficient of a two-dimensional electron gas in SrTiO3 *Nat. Mater.* 6 129-34.
[40] Nakajima A, Sumida Y, Dhyani M H, Kawai H, Narayanan E S 2010 High density two-dimensional hole gas induced by negative polarization at GaN/AlGaN heterointerface *Appl. Phys. Express* 3 121004.
[41] Al Mustafa N, Granzner R, Polyakov V M, Racko J, Mikolášek M, Breza J, Schwierz F 2012 The coexistence of two-dimensional electron and hole gases in GaN-based heterostructures *J. Appl. Phys.* 111 -.
[42] Nakajima A, Liu P, Ogura M, Makino T, Nishizawa S-i, Yamasaki S, Ohashi H, Kakushima K, Iwai H 2013 Temperature-Independent Two-Dimensional Hole Gas Confined at GaN/AlGaN Heterointerface *Appl. Phys. Express* 6 091002.
[43] Cutler M, Mott N F 1969 Observation of Anderson Localization in an Electron Gas *Phys. Rev.* 181 1336-40.

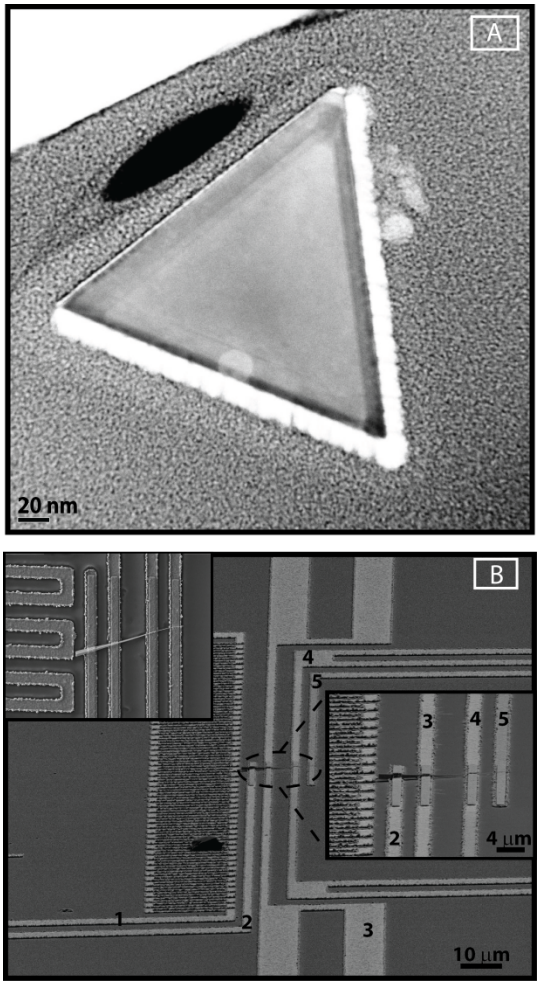

Figure 1 A: Cross-section STEM image of GaN/AlGaN core/shell NW. Darker region around the NW is the AlGaN layer. B: SEM image of our thermoelectric characterization platform. Right inset: zoom-in region showing a GaN/AlGaN nanowire suspended on the 4 metal contacts. Left top inset: SEM top view of the same device measurements while lead 1 is the heater for thermoelectric voltage measurements.

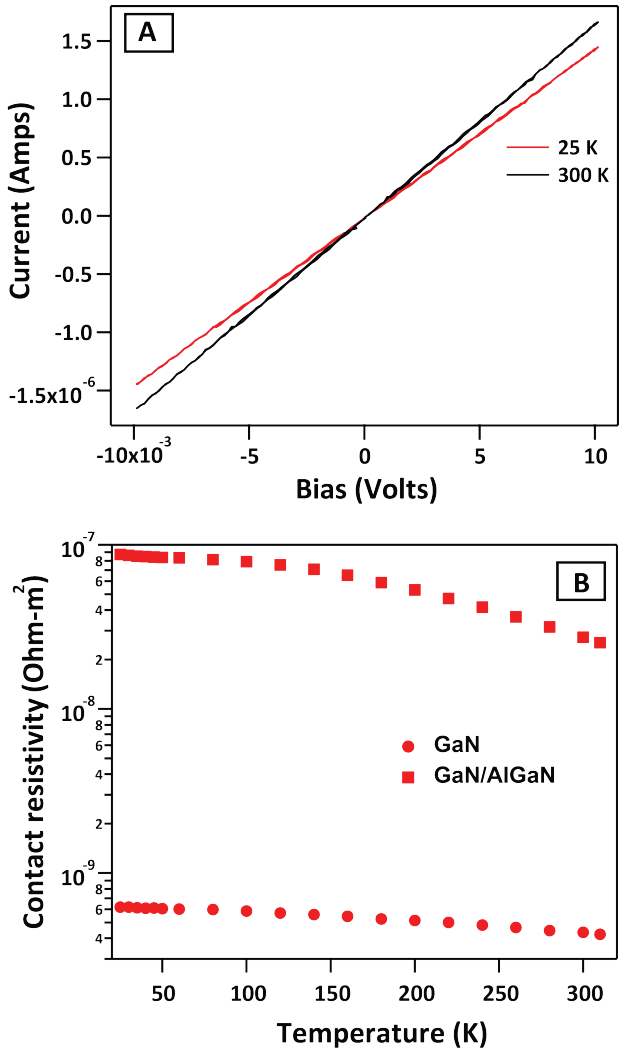

Figure 2. A: source-drain current at different temperatures as function of DC bias applied between contact 3 and 4 (Figure 1B). B: Contact resistivity as function of temperature for GaN and GaN/AlGaN nanowires after annealing at 750 °C in forming gas for 30 seconds.

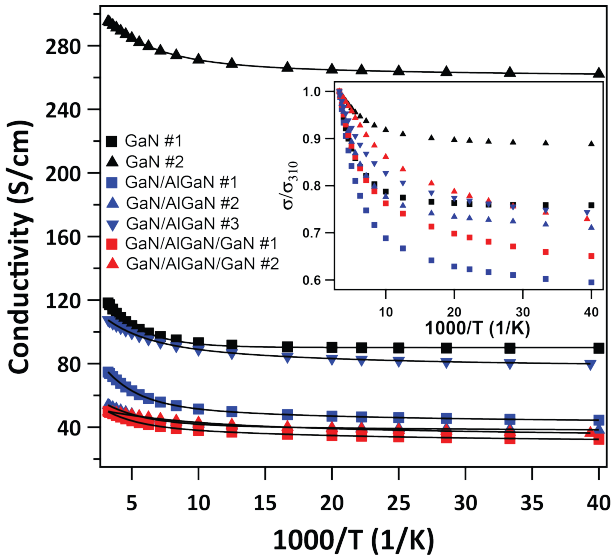

Figure 3. Electrical conductivity (σ) versus 1000/T. The solid lines represent the fitting of experimental data using the equations described in the text. Fitting parameters are shown in table 1. Inset: normalized conductivity versus 1000/T.

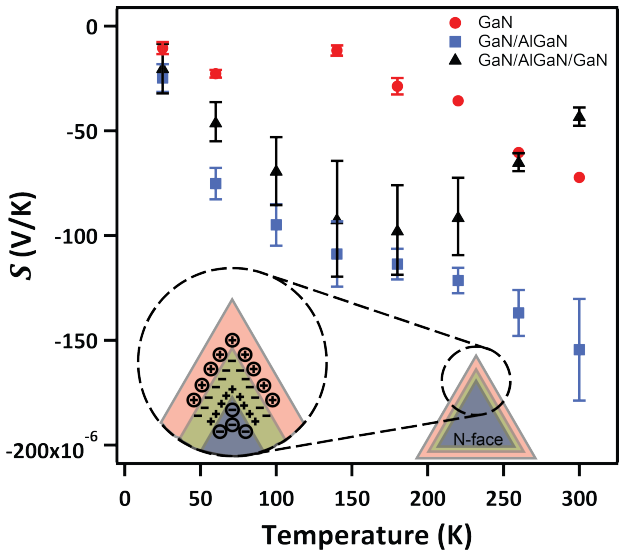

Figure 4. Measured Seebeck coefficient versus T. Inset: Schematic charge distribution of GaN/AlGaN/GaN core/shell/shell nanowire. Charges in circles represent either EG or HG while the others are polarization charges.